JOURNAL OF MATERIALS SCIENCE 12 (1977) 2281–2290

Thickness dependence of G_c for shear lip propagation from a single crack propagation specimen: aluminium 6061-T6 alloy, cold-rolled copper and BPA polycarbonate

R. P. KAMBOUR, S. MILLER*
General Electric Company Corporate Research and Development, Schenectady, New York, USA

Values of G_c for ductile crack propagation in a series of double cantilever beam specimens, each with a single side groove of constant depth, increase linearly with net section thickness. If a single side groove with linearly varying depth is cut in a double cantilever beam specimen, the tapered net section thickness results in a plastic zone, the cross-section area of which increases linearly with crack length. The attendant G_c increases in proportion to the plastic zone size in such a specimen. A single properly designed tapered section specimen appears to be capable of providing estimates of (a) the dependence of shear lip G_c on shear lip width, (b) the natural shear lip width and shape, and (c) the shear lip plastic strain.

G_c and plastic zone data from specimens of both kinds are reported for aluminium 6061–T6 alloy, cold-rolled copper and BPA polycarbonate. Results of uniaxial tensile tests and of centre-notch tensile tests are also reported for comparison purposes. G_cs, plastic zone sizes and plastic zone strains vary from material to material and appear to reflect in part the drawing and necking characteristics seen in uniaxial tensile tests.

1. Introduction

The thickness at which plane strain failure begins at the base of the groove is of considerable interest. In a series of ungrooved specimens of a given material G_c is understood [1] to reach a maximum and begins to decline when, with increasing thickness, plane strain failure begins in the interior of the specimen. However, the ability to predict the thickness at which plane strain failure begins is at present limited. This is particularly true with thermoplastics, in which the plastic zone at the plane-strain crack tip is made up of crazes while the plane stress zone involves shear deformation. The size of the shear lip thus depends on the crossover of the stress loci for two very different processes: (a) craze fracture and (b) shear yielding.

Recent studies [2, 3] of the mechanics of crack propagation in single groove double cantilever beam (SG DCB) specimens of BPA polycarbonate suggest that they give values of G_c that approximate the G_cs for shear lip formation. The attendant plastic zones are similar to shear lips in size, shape and plastic strain. Plastic zone cross-section area, and thus G_c is found to increase linearly with thickness of the net section between the base of the side groove and the opposite ungroove face. Plastic strain within the zone is found to be 30% independent of thickness. G_cs and plastic zone characteristics differ markedly from the corresponding parameters obtained from Dugdale tests on notched tensile specimens.

Characterization of the thickness dependence of G_c in SG DCB specimens is most obviously done by testing a series of specimens each of

* Present address; Major Appliance Business Group, Plastics Laboratory, Appliance Park, Bldg. 35, Rm. 1113, Louisville, Kentucky 40225, USA

which has a constant net section thickness. In this method the thickness at which plane strain failure begins at the root of the notch can be found only by enlarging the series to bracket the critical thickness closely. This approach is straightforward but wasteful of time and materials. A possible economical alternative utilizes a single specimen, the side groove of which is cut to a depth that varies linearly with distance along the long axis of the specimen. Fig. 1 shows two specimens of this kind having side grooves with a slit profile and a V-profile respectively. In each of these examples the groove depth varies from 100% of specimen thickness at a point 2 in. or so beyond the loading axis to zero at a point near the further end of the specimen. If the total length of specimen is 12 in. and the thickness is 0.2 in. the rate of increase of net section thickness is thus 0.02 in. in.

We have found that properly designed specimens of this kind can give linearly increasing values of G_c. At a given thickness the value of G_c obtained is essentially the same as that determined from a specimen of equal but constant net section thickness. Plastic zone cross-section areas, shapes and strains are identical at equivalent thicknesses as well. Finally when the groove is a thin flat slit and the specimen thickness is great enough, plane-strain failure appears to begin at a net section thickness that corresponds to the shear lip width in mixed mode failure.

The remainder of this paper reports experimental results obtained on BPA polycarbonate, an aluminium alloy, and cold-rolled copper to support the above conclusions. With aluminium and polycarbonate values of G_c have been contrasted to those obtained from the failure of centre-notched (CN) tensile specimens. Data from such specimens vary from one material to the next in ways that parallel certain plastic flow characteristics seen in uniaxial tensile behaviour.

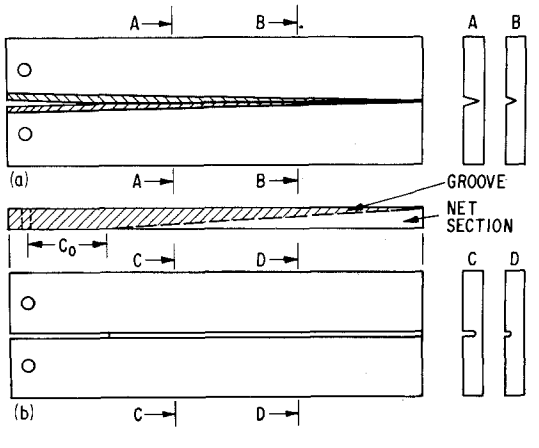

Figure 1 SG DCB specimens with tapered net section thickness and grooves that are, (a) V shaped, and (b) parallel-sided. Dimensions not to scale.

2. Materials

2.1. BPA polycarbonate

The BPA polycarbonate SG DCB specimens were cut form as-received extruded sheets of Lexan* 9034 resin of thicknesses up to 0.500 in. Two kinds of grooves were tested: V-profile grooves with roots 0.001 in. in radius and parallel-sided grooves with 0.005 in. radius bases. Buckling was countered with a yoke as before [1]. General yielding was delayed to greater net section thicknesses by using specimens of greater total thickness.

Tensile tests of centre-and edge-notched specimens were carried out on extruded film and sheet of thicknesses from 0.001 to 0.250 in. A standard uniaxial engineering stress-strain curve for polycarbonate is given in Fig. 2 for contrast purposes.

2.2. Aluminium

Sheets and H-beams of ALCOA aluminium alloy 6061–T6 were used. Sheet thicknesses ranged from 0.026 to 0.150 in. The H-beams were of two sizes: the smaller had a web 0.180 in. thick by 2 in. high with flanges $2\frac{1}{3}$ in. wide; the larger had a web 0.510 in. by 4 in. and flanges 3.25 in. wide. An engineering stress–strain curve for a specimen cut from the 0.150 in. sheet is shown in Fig. 2.

SG DCB specimens 3 in. wide and 12 in. long were fashioned from the 0.150 in. sheet. The side grooves were V-shaped with a 0.005 in. radius base. Buckling and general yielding were greater problems with these specimens than with polycarbonate sheet. The use of the H-beams eliminated lateral buckling and delayed general yielding to a greater net section thickness. CN tensile specimens 7 in. wide and 12 to 18 in. long were fashioned from a few of the thinner sheets and tested successfully.

2.3. Copper

Annealed OFHC copper strip† was cold-rolled from 0.0200 in. to 0.135 in. in several passes. The strip was subsequently milled to remove surface scale and produce a uniform thickness (~0.125 in.). Tensile tests were run on specimens cut perpen-

* Registered trademark of the General Electric Co.
† Copper Dev. Ass. No. 102

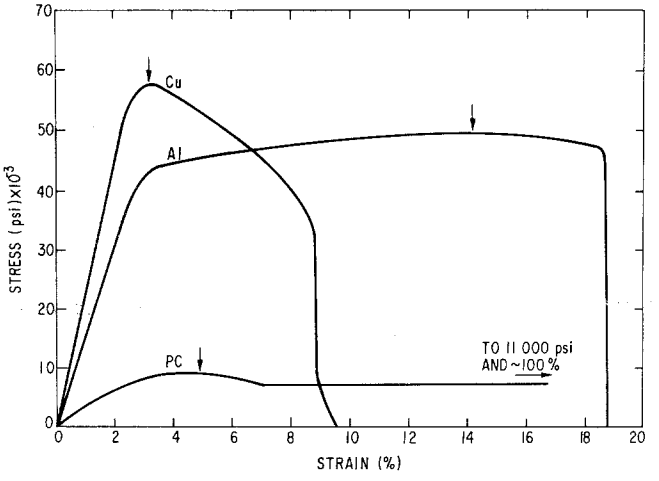

Figure 2 Aluminium 6061–T6, cold-rolled copper and BPA polycarbonate engineering stress–strain relationships. Metal gauge lengths = 1.1 in. (Al) and 1.2 in. (Cu) At fracture plane $\lambda = 1.90$ (PC), 1.80 (Al) and 3.80 (Cu).

dicular to the rolling direction (Fig. 2). Four SG DCB specimens of copper were tested for purposes of comparison with the other materials. Each copper SG DCB specimen was 12 in. long by 4 in. wide and had a V-groove with a 0.005 in. radius base. Buckling was a more serious problem with the copper specimens than with those of either of the other materials, and was reduced in specimens of constant net section thickness with the same yoke as was used with polycarbonate. In an alternative attempt to counter buckling, flanges 1.5 in. wide were electron-beam welded to one of the specimens before cutting the tapered groove. Because the width of the cold-rolled strip was only four inches, no attempt was made to fashion and test CN tensile specimens of copper.

3. Procedures

3.1. Mechanical tests

All DCB specimens were tested in an Instron Universal Tester at a constant crosshead speed (0.05 in. min^{-1}.) During each SG DCB test the distance a from the loading pins to the tip of crack at the ungrooved surface and the distance z from the loading pins to the visible tip of the plastic zone on the ungrooved surface were recorded at appropriate intervals. Crack and zone tip positions were easily determined in polycarbonate because of its transparency and the sharply bounded plastic zone. With the metals these positions were more difficult to fix due to opacity and the indistinct elasto–plastic boundary. This problem of plastic zone size in the metals tends to produce serious analytical errors, as will be discussed at length subsequently.

In the metals, determination of crack tip positions was made easier by shining a microscope light at the crack tip on the grooved side of the specimen and viewing from the ungrooved side. This was also very useful with the double-grooved large aluminium H-beam used for G_{Ic} determination.

With double-grooved DCB aluminium H-beam specimens used for G_{Ic} determination the desired, sharp 'starter' crack was generated from the initial through-thickness sawcut by fatigue cycling. The application of saturated sodium chloride solution to the base of the sawcut aided the formation of the starter crack. Subsequent to crack initiation the crack was washed and dried out before making the G_{Ic} determination.

Shear lips in aluminium were produced using the large H-beam. An attempt to drive a sharp crack into an ungrooved portion of the H-beam was frustrated by general yielding. Subsequently a section of the web of the beam was converted into a three point bend specimen of lateral dimensions 2.5 in. x 9 in. A mixed-mode crack was propagated across the 2.5 in. dimension of the specimen from a 0.5 in. long sawcut sharpened by corrosion fatigue.

3.2. G_c calculations

With stationary state crack propagation, G_c can generally be calculated [4] from

$$G_c = \frac{f^2}{2}\frac{d(\delta/f)}{dA} = \frac{\delta^2}{2}\frac{d(f/\delta)}{dA} \qquad (1)$$

where f is the applied force, δ the crosshead displacement, c the crack length and A the net

section area already cracked. In conventional DCB specimens, where the net section thickness w is constant,

$$G_c = \frac{f^2}{2w}\frac{d(\delta/f)}{dc} = \frac{\delta^2}{2w}\frac{d(f/\delta)}{dc}. \quad (2)$$

Hence

$$G_c = nf\delta/2wc \quad (3)$$

since $f/\delta = \alpha c^{-n}$ usually [5], where α is a constant dependent on modulus and beam geometry and n empirically determinable constant <3.

With polycarbonate SG DCB specimens of constant w, the use of the crack length a on the ungrooved surface for c in Equation 3 led to values of G_c that decreased with crack length [1]. Setting $c = z$, the distance to the plastic zone tip, in Equations 2 and 3 resulted in values of G_c that were independent of crack length on the average. This procedure was justified on the basis that, (a) the crack front at the surface lags behind that at the base of the groove and, (b) the plastic zone is generally considered to make the effective crack length greater than the geometric crack length.

The question of effective crack length has added importance in the case of our tapered net section specimens since

$$w = f(c) = \beta(c - c_0) \quad (4)$$

where $\beta \simeq 0.02$ and $c_0 \simeq 2$ in. The sensitivity to choice of c is greatest of course when values are extrapolated to $w = 0$. We generally find

$$\lim_{w \to 0} G_c \begin{cases} >0 \text{ if } c = a \\ <0 \text{ if } c = z \end{cases} \quad (5)$$

(This presumably reflects the fact that the plastic work done in a given transverse section begins before the crack tip at the groove base has reached this section and is finished only when the crack tip at the ungrooved surface has passed through the section.)

The linearity of G_c with w and the closeness of match between G_cs from tapered-w and constant-w specimens also depend on the choice of c. Maximizing the fit with constant-w G_cs sometimes brings finite extrapolated values of G_c at $w = 0$. This will be examined further in the discussion of results.

With constant-w DCB specimens the value of n in Equation 3 is always <3. Berry's studies [5] of polystyrene and polymethyl methacrylate showed that dummy specimens containing sawcuts in place of cracks, and the DCB specimens themselves, yielded identical values of n. We find that in constant-w SG DCB specimens of the ductile materials under study that Equation 3 still holds, but that the values of n obtained are larger by roughly 0.5 than the values obtained from dummy specimens containing sawcuts. Presumably the large crack-tip plastic zones are responsible.

With tapered-w specimens Equation 3 no longer holds. The form of the f/δ versus c relationship seems to vary with β and c_0. Recourse to Equation 2 with graphically determined values of $d(f/\delta)/dc$ produces values of G_c that accord well with G_cs from constant-w specimens in most cases. The fit is best when c in Equations 2 and 5 is set equal to $(a + z)/2$.

4. Results for polycarbonate

G_c versus w for three tapered groove specimens of polycarbonate is shown in Fig. 3. For one of these, c was set equal to $(a + z)/2$ in Equations 2 and 4; in Fig. 4 these data are plotted against $w_{(a+z)/2}$ (the subscript here denotes the choice of c in Equation 4). G_cs have been generated with both a and z in Equations 2 and 4 and in Fig. 4 plotted versus w_a and w_z, respectively. Finally, G_cs from several specimens of constant w have been entered for comparison purposes.

The three methods of treatment of tapered-w data give results that accord with those from constant-w specimens to varying degrees. However, G_cs for the tapered-slit specimen extrapolate to finite values at $w = 0$ regardless of whether a, z or $(a + z)/2$ is used. This presumably arises from the substantial width of the slit base, an effect seen before with constant-w specimens in which the groove bases were 0.020 in. wide [2]. The V-groove specimen data extrapolate to positively or negatively finite values of G_c depending on whether w_a or w_z is used. Use of $(w_c + w_z)/2$ results in extrapolation to zero at $w = 0$.

Tapered V-groove specimens, however failed to develop any sign of plane strain failure even when w was greater than 0.100 in. Two tapered slit specimens of total thicknesses 0.500 and 0.200 in. showed the onset of plane strain failure at the groove bases at $w \simeq 0.050$ and 0.100 in. respectively. In the first of these, catastrophic high-speed

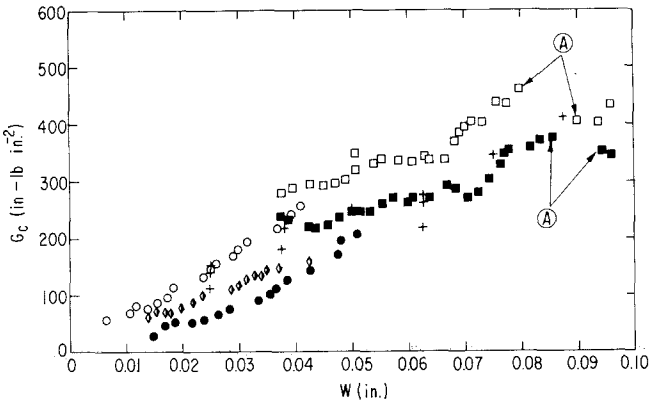

Figure 3 BPA polycarbonate: G_c versus w for SG DCB specimens of constant and tapered net section thicknesses. Key: Tapered slit specimen squares; 2 tapered V groove specimens circles and diamonds; 10 constant-w specimens + [1] $c = a$ open symbols; $c = (a + z)/2$ half-filled; $c = z$ filled. Mixed mode failure began between points marked A.

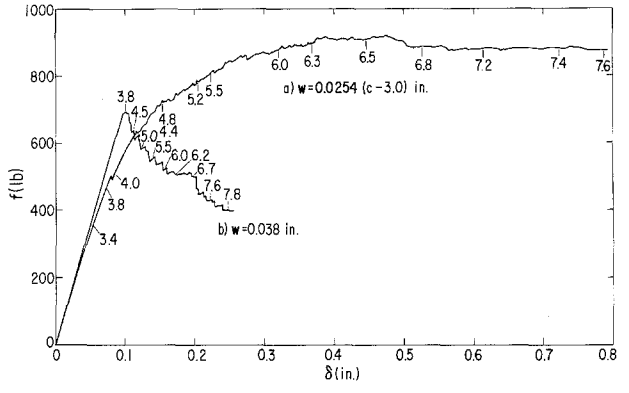

Figure 4 Aluminium 6061–T6: load–crosshead displacement traces for H-beam SG DCB specimens with (a) tapered and, (b) constant net section thicknesses. Numbers indicate crack lengths in inches at specimen surfaces.

failure resulted, the plane stress region of failure being reduced to a width of 0.001 to 0.002 in. In the other case (points labelled A in Fig. 4), low-speed mixed mode propagation occurred with a lower average G_c and a correspondingly somewhat smaller plane stress zone.

5. Results for aluminium 6061–T6

5.1. Mixed mode failure

Each of the shear lips in the 3-point bend aluminium specimen approached 0.23 in. in width assymptotically with distance from the starter crack, leaving a central plane strain fracture surface 0.050 in. wide. Each shear lip formed by slant fracture, the crack plane meeting the surface close to the boundary of the plane stress shear zone.

5.2. G_{Ic} and SG DCB G_cs

Crack propagation in all DCB and tensile specimens of aluminium proceeded irregularly with very audible 'pinging' and small but abrupt drops in load. Load-crosshead displacement traces for H-beams with constant and tapered net section thicknesses are reproduced in Fig. 4. Values of surface crack length are noted at intervals. The approximate constancy of load over large changes in crack length and displacement in the tapered specimen arises from a fortuitous balance between the dependence of w (and thus G_c) on crack length and the increase in beam compliance with length*.

Values of G_c from five constant-w SG DCB specimens are plotted against w in Fig. 5. Values of G_c from the tapered-w H-beam calculated and plotted using $c = (a + z)/2$ and the corresponding thicknesses $w_{(a+z)/2}$ are also shown. (Dashed and dotted lines show the loci of these data when a and z are used instead of $(a + z)/2$.) The value of G_{Ic} (horizontal line) obtained from the doubly grooved DCB H-beam compares well with G_{Ic} values obtained elsewhere [6].

With the SG DCB specimens, the dependence of G_c on w is again linear. Agreement between the constant- and tapered-w results would have been optimized slightly better by choosing values for c between a and $(a + z)/2$. Such a choice would have led to an extrapolated value of G_c at zero thickness of about 50 in.-lb in^{-2}†. Such a limiting value likely reflects the finite size of the plastic zone at

* For intervals where f is constant, G_c is easily shown to be given by $f(d\delta/dc)/2\beta(c - c_0)$, but this expression has not been used for G_c calculations.

† 1 in.-lb $\simeq 6.15 \times 10^{-2}$ J

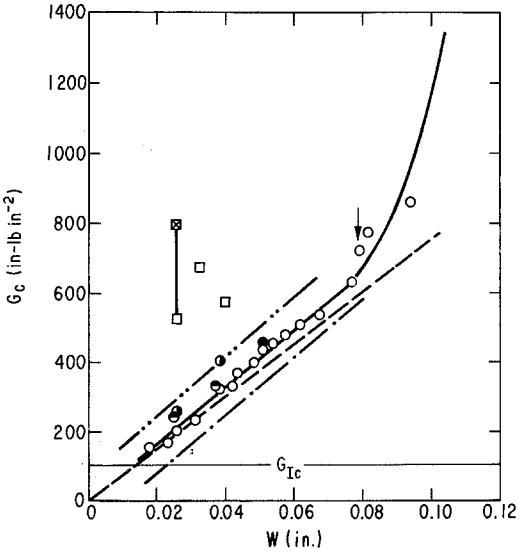

Figure 5 Aluminium 6061–T6: G_c versus w for SG DCB (circles) and CN tensile (squares) specimens. Tapered-w H-beam using $c = (a + z)/2$ ○. Constant-w H-beam ●. Constant-w sheet 0.150 in. total thickness ⊖. Dugdale G_c ⊠ G_c = yield stress times area in Fig. 8b □. Locus of tapered-w data when; $c = z$ –·–·–, $c = a$ –··–··–, and $c = (z + a)/2$ –●–. $G_c = \bar{\sigma}_y l_0 (\lambda - 1)$- - - -.

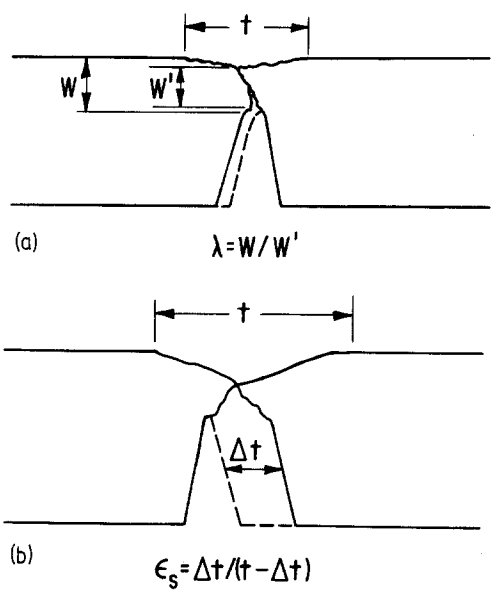

Figure 6 Cross-section profile of SG DCB specimen after testing with original V-groove profile shown (dotted line). (a) Aluminium 6061–T6, w = 0.36 in. (b) Cold-rolled copper, w = 0.49 in.

the root of the groove. This effect has already been discussed for polycarbonate specimens having substantial groove base sizes. Extrapolation of the SG DCB data to a thickness of 0.23 in. leads to an estimate of $G_c \simeq 2000$ in-lb in^{-2}. for the propagation of one shear lip, which is 20 times as large as G_{Ic}.

5.3. SG DCB plastic zones

Several of the SG DCB specimens, including the tapered groove H-beam, were sectioned with a band-saw normal to the crack direction. Photographs of groove bases in broken and untested sections were carefully compared in order to determine dimensional changes in the plastic zone (Fig. 6a). An extension ratio was calculated for the net section at the groove midplane as $\lambda = w/w'$ where w' is the net section thickness after fracture. The strain ϵ in the surface was also calculated by the method used previously with polycarbonate [2] and used here with the cold-rolled copper (see Fig. 6b). ϵ should equal $\lambda - 1$ if the assumptions underlying the two methods are correct. The 'gauge length' t_0 at the ungrooved surface, that becomes transformed into the plastic zone dimension t, was calculated by assuming that the extension ratio λ is constant throughout the yield zone. Thus $t = \lambda t_0$.

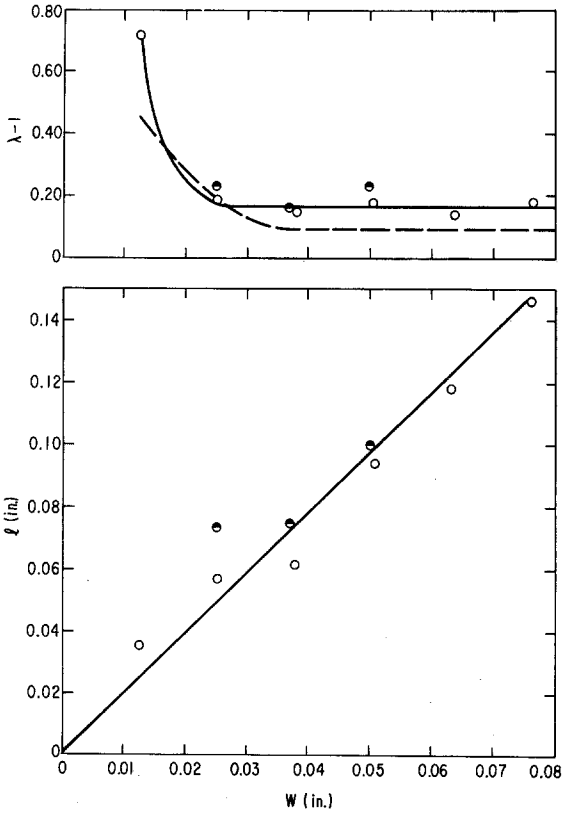

Figure 7 Aluminium 6061–T6: Dependence of l and λ on w for SG DCB specimens; Tapered-w H-beam ○, constant-w plates ⊖. Surface strain calculated as in Fig. 6b shown by dotted line.

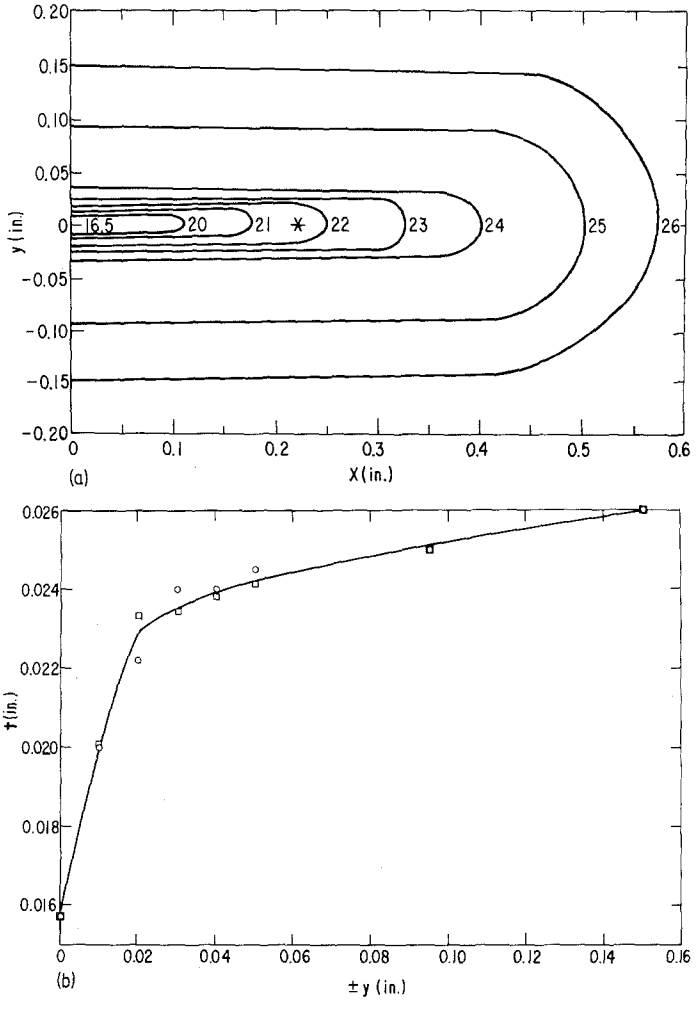

Figure 8 Aluminium 6061–T6 (a) Sheet thickness contours in the region beyond the crack tip in the 0.026 in. CN tension specimen. Crack tip is at $x = 0$, $y = 0$. Numbers give sheet thicknesses in mil. Average perceived zone tip position during test *. (b) Sheet thickness t versus distance above $(+y)$ and below $(-y)$ crack plane at $x = 0$.

The thickness dependence of these quantities is shown in Fig. 7. λ is constant for $w > 0.02$ in.; the plastic strain calculated as $1-\lambda$ is about 18% except for the thinnest sections and is similar to that at the boundary of the inner and outer parts of the CN tensile plastic zone (see below). The surface strain at large thicknesses has somewhat lower values (10 to 15%). In polycarbonate by contrast the SG DCB surface strain (30%) is about half that in CN tensile plastic zones [1], perhaps reflecting the greater sensitivity of flow processes in thermoplastics to hydrostatic components of stress.

$1-\lambda$ is greater than 17% for $w \leqslant 0.02$ in. As with G_c this rise appears to reflect the influence of the finite root radius, an effect seen in polycarbonate specimens with blunt grooves [2].

An independent estimate of G_c in SG DCB specimens has been formulated;

$$G_c \simeq \bar{\sigma}\bar{t}_0 (\lambda - 1) \qquad (7)$$

We set the effective stress $\bar{\sigma}$ at 52 000 psi,* rather than the uniaxial yield stress of 44 000 psi, in order to account for plane strain effects. The average gauge length $\bar{t}_0$ in the net section is set equal to half the surface gauge length, as was done previously with polycarbonate [1]. The resulting plot (dotted line Fig. 5) is about 90% of the experimental values of G_c. Had ϵ been used here the resulting plot would have been 50% of the experimental values.

5.4. G_cs from CN tensile specimens.

As with polycarbonate, positions of the crack and zone tips in the aluminium CN tensile specimens, as perceived by eye, were recorded as each test proceeded. Dugdale analyses were carried out in order to caluculate values of G_c.

Perceived zone-tip positions led to plots of s/a versus T/Y that departed substantially from theory. Here s is the zone length, a is s plus half

* 1 psi = 6.895×10^3 N m^{-2}

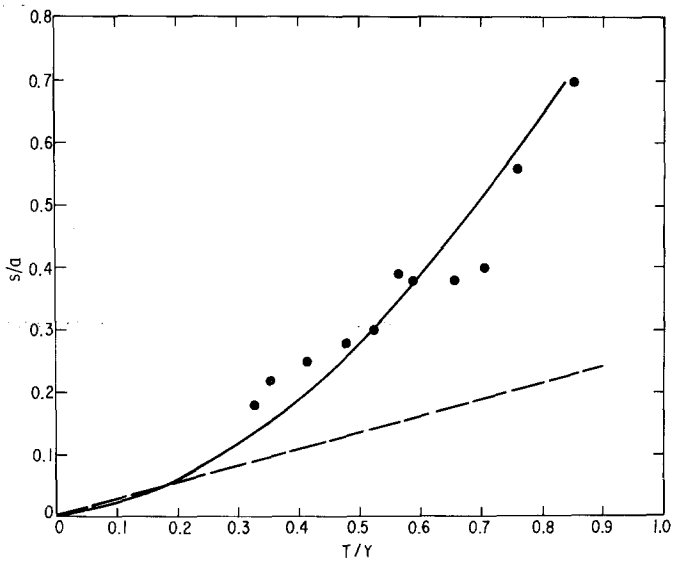

Figure 9 Aluminium 6061–T6: s/a versus T/Y where s has been increased by 0.35 in. to account for 'diffuse' yield region of plastic zone not evident to eye during tensile testing. Locus of data without s correction - - - -.

the crack length, T is the applied load and Y the yield load of the specimen. Subsequent determination of sheet thickness contours in the neighbourhood of crack tips showed that the plastic-zone boundary is much further from the crack tip than is perceived by eye (Fig. 8a). (That is, the yield zone can be divided into two parts; an outer diffuse part in which the strains are below 10 to 15%, and an inner concentrated-strain part in which the strain rises much more rapidly with distance (Fig. 8b). These parts are the analogues of the general yield and necking zones that develop before and after the point of maximum load (Fig. 2).)

Corrected values of s led to plots of s/a versus T/Y that followed theory [7] (Fig. 9). Values of G_c were calculated from

$$G_c = \frac{8\sigma_y^2 s_c}{\pi E}\gamma^2$$

where the stress for the yielding process σ_y was set equal to 45 000 psi. s_c is the zone length at maximum load, and E the modulus was set at 1×10^7 psi. The finite width correction factor γ was taken from Formann [8]. These G_cs are shown in Fig. 5 also.

An independent estimate of G_c for the 26 mil* thick CN specimen was made from the area above the curve in Fig. 8b and the yield stress. The value obtained (800 in-lb/in^2.) is larger thatn that given by the Dugdale calculation.

Finally it should be noted that slant fracture occured in all tensile and SG DCB specimens. In most specimens the slant angle alternated randomly from 45° above to 45° below the midplane roughly. With the tapered-groove H-beam the crack remained in the same slant plane throughout. The diffuse parts of the yield zones in CN tensile specimens are symmetrical with regard to the sheet plane; that is, the asymmetry that pre-figures the slant fracture develops only in the inner yield-zone. Deformation in the SG DCB plastic zone is also largely symmetrical with regard to the groove midplane (see Fig. 6a).

6. Results for cold-rolled copper

The cold-rolled copper SG DCB specimens were more difficult to test and gave less satisfactory results than the other materials. Two difficulties were encountered: most serious was the inablility to suppress plastic buckling sufficiently. In the constant-w specimens this took the form of out-of-plane bending of the beams on the axis lying in the net section. This bending occurred along the whole of the uncracked specimen length. The flanges on the tapered net section specimen prevented this deformation but did not prevent elastic buckling near the loading pins which in turn allowed an anti-plain character to develop in the crack-tip plastic zone. The failure of these copper specimens to behave properly reflects in part their G_cs which are apparently about four times as great as those in the aluminium specimens (see below).

The second difficulty was in determining the positions of the plastic zone tips. The lengths of the plastic zones were roughly 1 in. Although their

* 1 mil = 10^{-3} in.

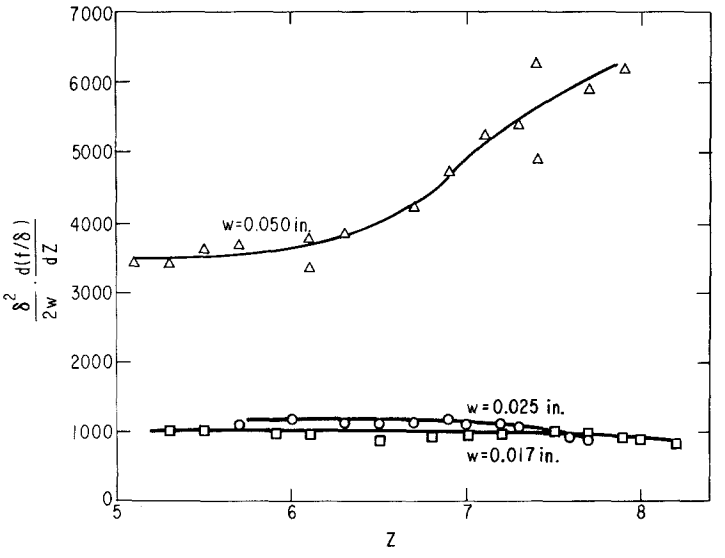

Figure 10 Cold-rolled copper: z dependence of $(\delta^2/2w)\ \mathrm{d}(f/\delta)/\mathrm{d}z$ for constant-w SG DCB specimens

boundaries parallel to the cracking direction were sharp (as with polycarbonate), their tips faded away gradually over a distance of as much as an inch, thus producing substantial uncertainties in the recorded value of z.

By contrast with Al 6061–T6 failure, the copper cracks proceeded smoothly. In the absence of anti-plain effects the yield zone developed symmetrically about the groove midplane, like polycarbonate but unlike the aluminium.

Values of $(f^2/2w)\,(\mathrm{d}(\delta/f)/\mathrm{d}z)$ are plotted versus z in Fig. 10 for the three constant-w specimens. The rise in level with increasing z that is evident with the thickest specimen can be attributed to plastic buckling in each beam behind the crack tip (an effect different from the net section buckling discussed above.) With this specimen G_c is therefore taken from the low z data in Fig. 10.

Fig. 11 contains the constant-w G_cs taken from Fig. 10 and results obtained from the tapered-w specimen calculated with and plotted against a. (The uncertainty in z mentioned above precluded the use of $(a + z)/2$).

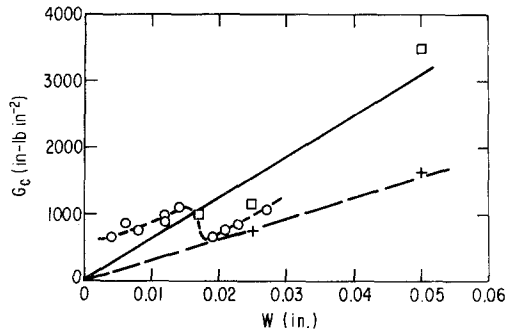

Figure 11 Cold-rolled copper: G_c versus w for SG DCB specimens of constant-w □, and tapered-w ○ with $c = a$. $1.15\sigma_y\Delta t/2$ for constant-w specimens +.

Cross sections were cut through the constant-w specimens and photographed. The plastic-zone size t on the specimen surface, the plastic strain ϵ at the surface and the surface plastic displacement Δt were determined from the photomicrographs (Fig. 6b). Again ϵ appeared to be constant (40%) but t increased roughly linearly with w.

The plastic work to failure was alternatively estimated as before, from $1.15\sigma_y\ \Delta t/2$, where $1.15\sigma_y$ is the presumed plane strain yield stress and σ_y is taken from Fig. 3 as 57 000 psi. The locus thus calculated is also entered in Fig. 11.

Although internal consistency is not very good, the results in Fig. 11, taken together, indicated that $\mathrm{d}G_c/\mathrm{d}w$ is roughly four times as great as with Al 6061–T6. Two factors obviously accounting for most of this difference are the surface strains (41 versus 10 to 18%) and the yield stresses (57 000 versus 43 000 psi).

In three ways the behaviour of the polycarbonate SG DCB's is more like that of the cold-rolled copper used here than that of Al 6061–T6. Because of the yield behaviour of copper, and polycarbonate, (i.e. post-yield tensile engineering stresses being lower than the yield stresses) their SG DCB yield zones are sharply bounded. Their plastic zone strains are similar. Finally, the cracks propagate smoothly and in the groove midplane in both materials.

In another way the behaviour of polycarbonate is more like that of aluminium 6061–T6. The

SG DCB side groove serves to localize strain in a small gauge section in all three materials. This limitation has the severest consequences for the aluminium and polycarbonate specimens when viewed in the framework of uniaxial tensile ductility. Plastic deformation spreads through the whole test section of tensile specimens of these materials and this contributes heavily to uniaxial tensile work-to-break. In the cold-rolled copper tensile tests, most of the plastic work occurs in the localized neck. Thus, the strain localization caused by the groove in the copper SG DCB specimens is much less serious a limitation.

7. Conclusions

The results presented here and in previous papers indicate that properly designed SG DCB specimens can be well-behaved fracture mechanics specimens. In our experience those specimens of constant net section thicknesses are easier to fabricate and test, while those of tapered net section thicknesses, when properly made and tested, can give a wealth of data for a minimum consumption of material. The same linear dependence of G_c on w is found with each type of specimen. The single clear-cut advantage of the tapered-w specimen is its potential for developing mixed mode failure at large w, thus indicating shear lip sizes.

SG DCB data quality will be highest when gross section thickness is large and the proper flanges are attached. By hindsight grooves should be parallel-sided slits with their roots sharpened dead sharp to approximate crack edges; these features will bring the onset of plane strain failure at the groove base at the proper values of w. The sharpened groove base will minimize excess local plastic flow that otherwise tends to result in G_cs that extrapolate to finite values at $w = 0$.

SG DCB specimens are generally superior to conventional CN tensile specimens for simulating shear lip formation. Crack-tip plastic displacements of the latter specimens differ from those in shear lips. Moreover, CN tensile specimens of ductile materials are plagued by other problems; The largest of these are general yielding and the excessive loads at failure necessitated by the specimen widths required to prevent general yielding. Also our unpublished observations show that in some materials the CN tensile plastic zones at maximum load have not grown to their maximum, 'steady-state' sizes; as a result G_cs calculated from the Dugdale equation may be substantially lower than those to be associated with steady-state fully ductile crack propagation in a tensile specimen.

Acknowledgements

We are indebted to L. F. Coffin, D. Lee, J. G. Williams and R. Bucci for helpful discussions.

References

1. A. S. TETELMAN and A. J. McEVILY Jr., "A Fracture of Structural Materials," (Wiley, New York, 1967).
2. R. P. KAMBOUR and S. MILLER, *J. Mater. Sci.* **11** (1976) 823.
3. *Idem, ibid.* **11** (1976) 1220.
4. C. GURNEY and J. HUNT, *Proc. Roy. Soc.* **A299** (1976) 508.
5. J. P. BERRY, *J. Appl. Phys.* **34** (1963) 62.
6. R. BUCCI, ALCOA Technical Center, New Kensington, Pa., private communication.
7. J. N. GOODIER and F. A. FIELD, in "Fracture of Solids", Metallurgical Society Conference, Vol. 20, edited by D. C. Drucker and J. J. Gilman, (Interscience, New York, 1963) p. 103.

Received 7 January and accepted 18 February 1977